Research Square

Preprints are preliminary reports that have not undergone peer review.
They should not be considered conclusive, used to inform clinical practice,
or referenced by the media as validated information.

A case report about nonspecific chronic lymphadenitis associated AA amyloidosis nephrotic syndrome

Liangliang Zhang
Eighth Affiliated Hospital of Sun Yat-sen University
Ruo Wu
Sun Yat-sen University
Guodu Liu
Eighth Affiliated Hospital of Sun Yat-sen University
Minjia Feng
Sun Yat-sen University
Li Yin
yinli9@mail.sysu.edu.cn
Eighth Affiliated Hospital of Sun Yat-sen University
Aoran Huang
Eighth Affiliated Hospital of Sun Yat-sen University
Hui Huang
Sun Yat-sen University

Case Report

Keywords: Chronic lymphadenitis, AA amyloidosis, Nephrotic syndrome, PET-CT, Case report

Posted Date: November 24th, 2026

DOI: https://doi.org/10.21203/rs.3.rs-11214996/v1

License: This work is licensed under a Creative Commons Attribution 4.0 International License.
Read Full License

Additional Declarations: No competing interests reported.

Abstract

Introduction:

AA amyloidosis is mostly caused by chronic inflammatory diseases, malignant tumors or less common infectious diseases. A nonspecific chronic lymphadenitis associated AA amyloidosis nephrotic syndrome is seldom reported.

Case Summary:

A 56-year-old Chinese woman who presented with bilateral lower limb edema and was diagnosed with nephrotic syndrome. Renal biopsy confirmed AA amyloidosis based on Congo red staining and immunohistochemistry. A comprehensive workup excluded common secondary causes AA amyloidosis such as autoimmune disease, infection, and malignancy. Consequently, 18F-FDG PET-CT identified a metabolically active mesenteric soft tissue mass and enlarged lymph nodes. Laparoscopic lymph node dissection revealed chronic lymphadenitis with reactive follicular hyperplasia. Following surgical removal, the patient's edema improved, and her proteinuria and serum albumin levels gradually normalized over one year.

Conclusion

Advanced imaging such as PET-CT may be pivotal in detecting occult inflammatory sources when routine evaluations are inconclusive. Early identification and management of the underlying etiology can lead to significant clinical improvement.

Introduction

Amyloidosis results from the deposition of amyloid fibrils, which are composed of insoluble protofilaments that are resistant to proteolysis.[1] AA amyloidosis is a form of systemic amyloidosis caused by chronic inflammatory stimuli that lead to sustained production of serum amyloid A (SAA) protein and its subsequent deposition in tissues.[2] In response to inflammatory cytokines such as interleukin-1 (IL-1) and tumor necrosis factor-alpha (TNF-α), the liver produces large amounts of the acute-phase protein SAA.[3] This protein undergoes misfolding within macrophages, aggregates into β-sheet-rich amyloid fibrils, and deposits in the extracellular matrix.[4] SAA protein is mainly deposited in the kidneys, liver, spleen, etc. through blood circulation, among which kidney involvement is extremely common.[5] In the kidneys, SAA is mainly deposited in the glomerular mesangium, capillary basement membrane, arterioles, and tubular interstitium, destroying the normal structure of the glomerular filtration barrier and causing a large amount of protein to leak through the kidney.[6]

This case represents a rare instance of AA amyloidosis-associated nephrotic syndrome, with amyloid deposition confined exclusively to the kidneys and no involvement of other organs. The underlying cause of amyloidosis was identified as isolated chronic lymphadenitis—a highly unusual etiology. Notably, in that prior case, amyloid deposition was more widespread. In our case, the early use of PET-CT imaging allowed for prompt identification and surgical removal of the affected lymph node, which may have contributed to the patient's favorable prognosis.

Case presentation

A 56-year-old Chinese woman with no significant past medical history was admitted to the hospital in July 2022 with a one-month history of bilateral lower limb edema. She reported experiencing a "cold attack" approximately one month ago shortly after COVID-19 vaccination, without accompanying symptoms such as rash, arthralgia, erythema, or fever. Family history includes a sister with rheumatoid arthritis and a son with Graves' disease. Upon admission, laboratory investigations revealed significant proteinuria (8,464 mg/24 hours), elevated serum cholesterol (7.45 mmol/L), hypoalbuminemia (18.58 g/L), high C-reactive Protein (CRP) (55.95mg/L) and erythrocyte sedimentation rate (ESR) (95mm/1h), and normal serum creatinine (57.5 μmol/L). Based on these findings, nephrotic syndrome was suspected, .and a renal biopsy was performed for further evaluation. Meanwhile, A comprehensive workup was conducted to exclude other potential secondary causes of nephrotic syndrome. This included testing for vasculitis, some autoimmune profile, cytokines (such as tumor necrosis factor [TNF] and interleukins [IL]). Detailed laboratory examination results upon admission are shown in Supplementary Table 1.

Light microscopy of the renal biopsy specimen (47 glomeruli, 3 of which were globally sclerotic) revealed pink-stained, homogeneous, amorphous deposits in the mesangial areas of the remaining glomeruli. (Fig. 1) These deposits expanded portions of the mesangium and were associated with segmental "eyelash-like" changes in the glomerular basement membrane, along with compression of the capillary loops. Congo red staining of the deposits demonstrated characteristic apple-green birefringence under polarized light. While no obvious proliferation of parietal epithelial cells and no crescent formation were seen. Renal tubular epithelial cells exhibited vacuolar and granular degeneration, with some showing marked granular degeneration and prominent eosinophilic granules. The lumens of several renal tubules were dilated, the brush border was lost, and focal tubular atrophy was noted, involving approximately 5% of the sampled tissue. Mild interstitial fibrosis and focal inflammatory cell infiltration were present in the renal interstitium. Additionally, arteriolar walls appeared thickened.

Light microscopy of the glomeruli revealed amyloid deposits demonstrated by various staining methods: (a) Hematoxylin and Eosin (HE) stain, (b) Periodic Acid–Schiff (PAS) stain, (c) Periodic Acid–Silver Methenamine (PASM) stain, (d) Masson's trichrome stain, (e) Congo red stain, and (f) Alkaline Congo red stain. Original magnification ×100 in (a), ×400 in (b) to (f).

Electron microscopy revealed segmental thickening of the glomerular basement membrane and widespread effacement of foot processes. (Fig. 2) No electron-dense deposits were observed. Instead, abundant fibrillar material was identified within the mesangial regions and along the glomerular basement membrane. These fibrils measured approximately 8–12 nm in diameter, were rigid, non-branching, and displayed a randomly oriented, disorganized arrangement. Immuno-electron microscopy demonstrated no labeling with kappa or lambda light chains, as no colloidal gold particles were detected on the amyloid fibrils. In contrast, strong positive labeling was observed with serum amyloid A (AA), evidenced by extensive attachment of colloidal gold particles to the fibril, and immunohistochemical analysis confirmed that the deposits were composed of serum amyloid A (SAA) proteins.

Immuno-electron microscopy markers: (a)Kappa (-, no colloidal gold particles attached to amyloid fibers), (b) Lambda (-, no colloidal gold particles attached to amyloid fibers), (c) and (d) AA (+, a large amount of colloidal gold particles attached to amyloid fibers)

Then finding the cause of AA amyloidosis has become the most important task. Common autoimmune marker and tumor marker all showed negative results. (see supplementary table 2) Additionally, metagenomic next-generation sequencing (mNGS) was performed to detect potential DNA-pathogen microbial infections. Hereditary disorders were considered and whole-genome sequencing—revealed no significant abnormalities. Early diagnosis and effective treatment at a stage before renal function is irreparably damaged are key to improving the prognosis of patients with AA amyloidosis.[7] To early investigate potential occult inflammatory sources, a fluorine-18 fluorodeoxyglucose positron emission tomography-computed tomography (18F-FDG PET-CT) scan was performed.

The PET-CT revealed a 3.1 × 4.4 cm soft tissue mass in the mesenteric region of the abdominal cavity exhibiting increased metabolic activity. (Fig. 3) Additionally, mildly increased metabolic activity was observed in several lymph nodes in the uterine and retroperitoneal regions. Unifocal Castleman disease was initially considered, therefore laparoscopic lymph node dissection was performed, including removal of the enlarged node and several surrounding lymph nodes, for determination of the pathology.

High 18F FDG uptake in the arrowed area, size is approximately 3.1×4.4cm, and the enhanced scan shows uniform enhancement. Multiple punctate/sheet-like calcifications are seen inside, with clear boundaries and smooth edges, and no clear correlation with surrounding organs.

Lymph node biopsy revealed preserved normal architecture of the cortex, medulla, and lymphatic sinuses. Reactive follicular hyperplasia was observed within the cortex and medulla. Focal areas in the interstitium showed vascular proliferation with hyaline degeneration. Dilated lymphatic sinuses were noted, accompanied by plasma cell aggregation. (Fig. 4) Immunohistochemical staining showed the following results in Table 1. Overall, the findings are consistent with chronic lymphadenitis with reactive follicular hyperplasia.

Panels (a)–(d) show sections stained with hematoxylin and eosin (HE), while panels (e) and (f) show immunohistochemical staining for CD38.

Table 1
Immunohistochemistry, and In Situ Hybridization Findings

Pathological Features	Result
Immunohistochemistry	
CD20	Positive in follicles
CD5	Positive in interfollicular areas
CD38	Positive in interfollicular plasma cells
CD10	Positive in germinal centers
Bcl-2	Negative in germinal centers
HHV8	Negative
IgG	~ 250 cells/HPF
IgG4	~ 30 cells/HPF
Ki-67	~ 15% positive in interfollicular area
In Situ Hybridization	
EBERs (EBV-encoded RNA)	Negative

Bcl-2: B-cell lymphoma 2, HHV-8: Human Herpesvirus 8, Ki-67: Ki-67 antigen, EBERs: Epstein–Barr virus-encoded RNAs

Clinical Timeline of the Patient's Diagnostic and Therapeutic Course

Timeline of the patient’s clinical course, including initial admission for nephrotic syndrome (July 30, 2022), renal biopsy confirming amyloidosis (August 3, 2022), detection of retroperitoneal lymphadenopathy by PET-CT (August 2022), and surgical excision of the lymph node confirming lymphadenitis (September 13, 2022).

Clinical outcome

Clinical outcome

A comprehensive evaluation was conducted to assess potential involvement of other organs by amyloid deposition. Transthoracic echocardiography showed normal interventricular septum and left ventricular posterior wall thickness. Electrocardiography revealed no low voltage in limb leads. Random gastrointestinal biopsies were negative for Congo red staining. Electromyography and nerve conduction studies were within normal limits, and cranial CT imaging showed no abnormalities. No extra-renal organ involvement was found, and following surgery the patient's bilateral lower limb edema significantly

improved. In terms of medication, only symptomatic supportive treatment such as albumin supplementation was provided. One year later, her proteinuria had decreased to 3,103 mg/24 hours and erythrocyte sedimentation rate had fallen to 42mm/1h. At the clinical follow-up visit in May 2024, the 24-hour urinary protein further declined to 2,535 mg/24 hours, and her serum albumin level had normalized to 40.17 g/L.

Discussion

The case presented in this article is a Chinese female with nephrotic syndrome caused by chronic lymphadenitis related AA amyloidosis with plasma cell interfollicular infiltration. Following surgical resection of the affected lymph nodes, the patient's clinical condition as bilateral lower limb edema improved significantly over a three-year follow-up, with progressive reduction in proteinuria and normalization of serum albumin levels. In this case, we report a newly identified instance of lymphadenitis-associated AA, in which early application of positron emission tomography (PET) imaging facilitated prompt identification of lymph node pathology. This early diagnostic insight enabled timely intervention, leading to a favorable clinical outcome. To our knowledge, this is among the first documented cases where PET imaging played a pivotal role in the early detection of lymphadenitis caused AA, underscoring its potential value in guiding diagnosis and improving prognosis in similar atypical presentations.

Although nephrotic syndrome is a common phenotype of AA amyloidosis, it is not common among all causes of nephrotic syndrome.[8] Also, AA amyloidosis is a minority of amyloidosis. In an epidemiological review of 474 cases of renal amyloidosis, 86% were Ig-related (mainly AL type) and only 7% were AA type.[9] AA amyloidosis causes a greater degree of renal dysfunction than AL amyloidosis and tends to affect younger individuals.[10] In addition to kidney involvement, the digestive system, heart and nervous system may also be affected.[11–13] In this case, renal involvement was the only manifestation of amyloid deposition. Within the short span of one month, the patient developed extremely severe proteinuria, reaching 8,464 mg/24 hours. Despite this marked protein loss, serum creatinine levels remained consistently within the normal range throughout the disease course. This discrepancy suggests that glomerular injury occurred without significant tubular or interstitial damage, which may indicate early-stage amyloid involvement predominantly limited to the glomeruli. The preservation of renal filtration function despite heavy proteinuria underscores the importance of early detection and intervention in such cases.

The origin of chronic lymphadenitis in this case remains unclear. Upon taking a detailed medical history, the only noted symptom was a self-limited “cold” episode approximately one month prior to the onset of lower limb edema. No prolonged fever or other systemic signs, such as hepatosplenomegaly or cardiovascular involvement, were present. On the one hand, the patient's family history raises the possibility of an underlying autoimmune predisposition. Her sister has a known diagnosis of rheumatoid arthritis, and her son has a history of Graves' disease—both autoimmune conditions. Although the patient herself showed no clinical or serological evidence of systemic autoimmune disease, this

clustering of autoimmune disorders within the family suggests a potential genetic susceptibility that might have contributed to the chronic lymphadenitis or the development of AA amyloidosis. Another noteworthy factor is the administration of a COVID-19 vaccine approximately one month prior to symptom onset. While transient lymphadenopathy has been well-documented as a benign and self-limited side effect of COVID-19 vaccination, retroperitoneal lymphadenopathy is rare but has been reported[14]. On the other hand, viral upper respiratory infections (“cold”) are well known to cause transient reactive lymphadenopathy, particularly in cervical regions, as part of the immune response. However, such lymphadenopathy typically resolves within days to weeks and no article on “Pubmed” documented with chronic or deep-seated lymphadenitis, such as retroperitoneal involvement.

Although AA amyloidosis associated with nonspecific retroperitoneal lymphadenitis is extremely rare, there had been only one case report as early as the last century on Pubmed.[15] This article raised a question: Is AA amyloidosis always secondary? This case raises an important question: Is AA amyloidosis always secondary? In the absence of a clearly identifiable cause, this case may be categorized as idiopathic AA amyloidosis. Our case is even rarer than the documented case in that the amyloidosis caused by lymphadenitis in this patient was localized to the kidneys. Localized amyloidosis is rare in both AA and AL amyloidosis.[16] Interestingly, clinical condition of this patient significantly improved following surgical excision of the suspected lymph node, suggesting a causal relationship.

Treatment of AA amyloidosis focuses on controlling the primary inflammatory lesions (such as anti-rheumatic drugs, biological agents, anti-infective therapy) and concurrent renal protection therapy.[17] Current guidelines for the evaluation of AA amyloidosis focus primarily on identifying chronic inflammatory conditions but do not recommend the use of positron emission tomography (PET).[18] This may partly due to the high cost and radiation exposure, as well as the relatively low sensitivity in detecting underlying etiologies. Moreover, AA amyloid deposits are typically metabolically inactive and appear as cold nodules or areas of low uptake on PET-CT, limiting its utility in identifying sites of tissue involvement.[19] Nevertheless, in this case, early use of PET-CT led to the detection of an occult lesion, allowing prompt surgical intervention before disease progression. Other case reports have similarly described the successful use of PET-CT in managing AA amyloidosis.[20–22]

Progression to end-stage renal disease (ESRD) is common in patients with renal amyloidosis. In a French cohort study of 68 patients with AA amyloidosis, 38.2% progressed to ESRD during follow-up.[23] Another cohort in Italy showed 37 patients out of 78 with AA amyloidosis (47%) developed ESRD and had to begin a dialytic therapy.[24] However, some people believe that the prognosis of the disease is related to the location of SAA deposits. One study reported that up to 85% of patients with biopsy-proven glomerular disease progressed to renal failure, while this proportion was 0% in patients with vascular or tubular AA deposits.[25] Most cases of AA amyloidosis appear to develop slowly, but a small percentage of patients with familial Mediterranean fever present with acute onset, heavy proteinuria, elevated inflammatory markers, and rapid progression to renal failure within weeks. These rare cases have been described as "amyloid storms" and are thought to be triggered by superimposed infections.[26] Overall, our

patient achieved remarkable recovery, suggesting that early, aggressive diagnostic evaluation—particularly the use of PET-CT—may be instrumental in improving long-term renal outcomes in selected cases.

Declarations

Conflict of interest

The author states that this research was conducted without any commercial or financial relationships, which may be interpreted as a potential conflict of interest.

Funding

National Natural Science Foundation of China (82400859), Health and Wellness in Futian District, Shenzhen (FTWS095), Natural Science Foundation Shenzhen Basic Research Project (JCYJ20250604142502003) to Li Yin. Noncommunicable Chronic Diseases- National Science and Technology Major Project (2025ZD0547300), National Natural Science Foundation of China (82330021, 82270771), Shenzhen Science and Technology Program (KCXFZ20211020163801002, ZDSYS20220606100801004, SGDX20230116092459009), the Regional Joint Funding Key Project of Guangdong Basic Research and Basic Research for Application (2024B1515120018), and Shenzhen Key Medical Discipline Construction Fund (SZXK002), Futian District Public Health Scientific Research Project of Shenzhen (FTWS2022001), Chinese Association of Integrative Medicine-Shanghai Hutchison Pharmaceuticals Fund (HMPE202202), China Heart House-Chinese Cardiovascular Association HX fund (2022-CCA-HX-090) to Hui Huang.

Author Contribution

LLZ and HH contributed to the conception and design of the study. GDL, LLZ and LY wrote the first draft of the manuscript. MHL did the critical revision of the manuscript. All authors contributed to the article and approved the submitted version.

Acknowledgments

We thank the patients and their families for participating in this study.

Data availability

The original contributions presented in the study are included in the article Material. Further inquiries can be directed to the corresponding author.

Ethic statement

Written informed consent was obtained from the individual(s) for the publication of any potentially identifiable images or data included in this article.

References

1. Pepys MB, Amyloidosis. Annu Rev Med. 2006;57:223–41. 10.1146/annurev.med.57.121304.131243.
2. Karam S, Haidous M, Royal V, Leung N, Renal. AA amyloidosis: presentation, diagnosis, and current therapeutic options: a review. Kidney Int. 2023;103:473–84. 10.1016/j.kint.2022.10.028.
3. Lachmann HJ, et al. Natural history and outcome in systemic AA amyloidosis. N Engl J Med. 2007;356:2361–71. 10.1056/NEJMoa070265.
4. Yong HS et al. Primary localized amyloidosis manifested as supraclavicular and mediastinal lymphadenopathy. *The British journal of radiology* 80, e131-133. 10.1259/bjr/52539691 (2007).
5. de Real D, et al. Systemic AA amyloidosis: epidemiology, diagnosis, and management. Clin Epidemiol. 2014;6:369–77. 10.2147/clep.S39981.
6. Feitosa VA, Neves P, Jorge LB, Noronha IL, Onuchic LF. Renal amyloidosis: a new time for a complete diagnosis. Brazilian J Med Biol Res = Revista brasileira de pesquisas medicas e biologicas. 2022;55:e12284. 10.1590/1414-431X2022e12284.
7. Palladini G, et al. Prognostication of survival and progression to dialysis in AA amyloidosis. Amyloid: Int J experimental Clin Invest : official J Int Soc Amyloidosis. 2017;24:136–7. 10.1080/13506129.2017.1289917.
8. Zuckerman JE, Peng F, Karl BE, Schulze CE, Sisk A. Cancer-Associated AA Amyloidosis Presenting as Crescentic Glomerulonephritis. Kidney Int Rep. 2019;4:882–7. 10.1016/j.ekir.2019.02.017.
9. Said SM, et al. Renal amyloidosis: origin and clinicopathologic correlations of 474 recent cases. Clin J Am Soc Nephrology: CJASN. 2013;8:1515–23. 10.2215/cjn.10491012.
10. Panizo N, Rivera F, López-Gómez JM. Decreasing incidence of AA amyloidosis in Spain. Eur J Clin Invest. 2013;43:767–73. 10.1111/eci.12097.
11. Fushimi T, et al. Severe protein losing enteropathy with intractable diarrhea due to systemic AA amyloidosis, successfully treated with corticosteroid and octreotide. Amyloid: Int J experimental Clin Invest : official J Int Soc Amyloidosis. 2005;12:48–53. 10.1080/13506120500032725.
12. Reyners AK, Hazenberg BP, Reitsma WD, Smit AJ. Heart rate variability as a predictor of mortality in patients with AA and AL amyloidosis. Eur Heart J. 2002;23:157–61. 10.1053/euhj.2001.2972.
13. Bajic VP, et al. DES-Amyloidoses Amyloidoses through the looking-glass: A knowledgebase developed for exploring and linking information related to human amyloid-related diseases. PLoS

ONE. 2022;17:e0271737. 10.1371/journal.pone.0271737.

14. Kim DH, et al. Enlarged lymph node occupying the retroperitoneal space and psoas muscle causes ureteric compression and graft kidney hydronephrosis after COVID-19 mRNA vaccine booster: a case report. Clin transplantation Res. 2025;39:66–70. 10.4285/ctr.24.0027.
15. Maury CP, Törnroth T, Wegelius O. Is amyloid A (AA) amyloidosis always secondary? Ann Rheum Dis. 1985;44:273–6. 10.1136/ard.44.4.273.
16. Nin CS, et al. Thoracic lymphadenopathy in benign diseases: A state of the art review. Respir Med. 2016;112:10–7. 10.1016/j.rmed.2016.01.021.
17. Thorne J, et al. Serum Amyloid A Protein-Associated Kidney Disease: Presentation, Diagnosis, and Management. Kidney Med. 2022;4:100504. 10.1016/j.xkme.2022.100504.
18. Georgin-Lavialle S, et al. French practical guidelines for the diagnosis and management of AA amyloidosis. La Revue de Med interne. 2023;44:62–71. 10.1016/j.revmed.2022.12.004.
19. Glaudemans AW, Slart RH, Noordzij W, Dierckx RA, Hazenberg BP. Utility of 18F-FDG PET(/CT) in patients with systemic and localized amyloidosis. Eur J Nucl Med Mol Imaging. 2013;40:1095–101. 10.1007/s00259-013-2375-1.
20. Ihne S, et al. AA amyloidosis in inflammatory active malignant paraganglioma. Amyloid: Int J experimental Clin Invest : official J Int Soc Amyloidosis. 2022;29:137–8. 10.1080/13506129.2021.2016691.
21. Papathanasiou M, et al. (18)F-florbetaben positron emission tomography detects cardiac involvement in systemic AA amyloidosis. Eur J Nucl Med Mol Imaging. 2020;47:3186–7. 10.1007/s00259-020-04861-4.
22. Wang J, Zhao B, Song T, Sun J. Lung cancer combined with diffuse peritoneal and mesenteric amyloidosis detected on 18F-FDG PET/CT: A case report. Medicine. 2021;100:e25961. 10.1097/md.0000000000025961.
23. Verine J, et al. Clinical and histological characteristics of renal AA amyloidosis: a retrospective study of 68 cases with a special interest to amyloid-associated inflammatory response. Hum Pathol. 2007;38:1798–809. 10.1016/j.humpath.2007.04.013.
24. Bergesio F, et al. Renal involvement in systemic amyloidosis: an Italian collaborative study on survival and renal outcome. Nephrol dialysis transplantation: official publication Eur Dialysis Transpl Association - Eur Ren Association. 2008;23:941–51. 10.1093/ndt/gfm684.
25. Uda H, et al. Two distinct clinical courses of renal involvement in rheumatoid patients with AA amyloidosis. J Rhuematol. 2006;33:1482–7.
26. Kukuy OL, Beckerman P, Dinour D, Ben-Zvi I, Livneh A. Amyloid storm: acute kidney injury and massive proteinuria, rapidly progressing to end-stage kidney disease in AA amyloidosis of familial Mediterranean fever. Rheumatology (Oxford). 2021;60:3235–42. 10.1093/rheumatology/keaa772.

Figures

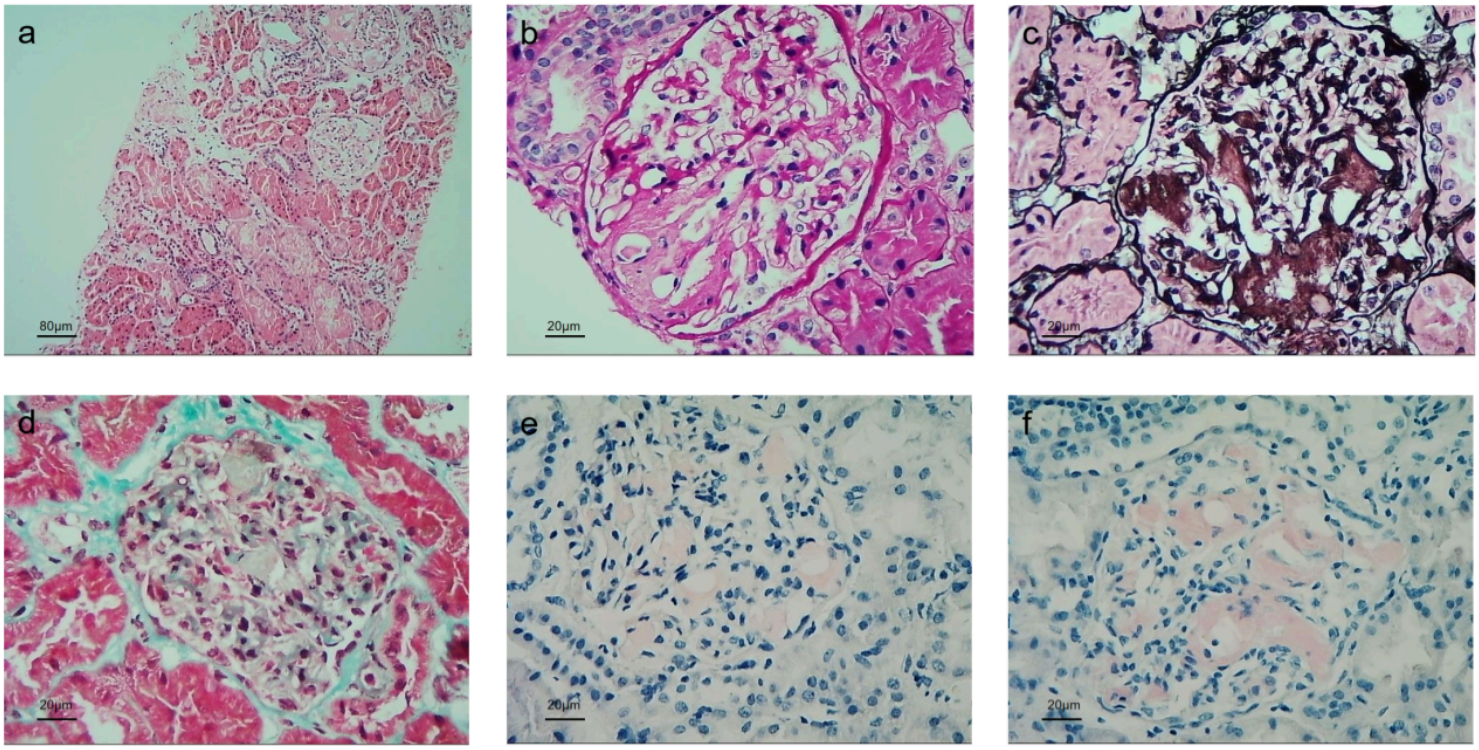


Figure 1

Light microscopy of the renal biopsy specimen

Light microscopy of the glomeruli revealed amyloid deposits demonstrated by various staining methods: (a) Hematoxylin and Eosin (HE) stain, (b) Periodic Acid–Schiff (PAS) stain, (c) Periodic Acid–Silver Methenamine (PASM) stain, (d) Masson's trichrome stain, (e) Congo red stain, and (f) Alkaline Congo red stain. Original magnification ×100 in (a), ×400 in (b) to (f).

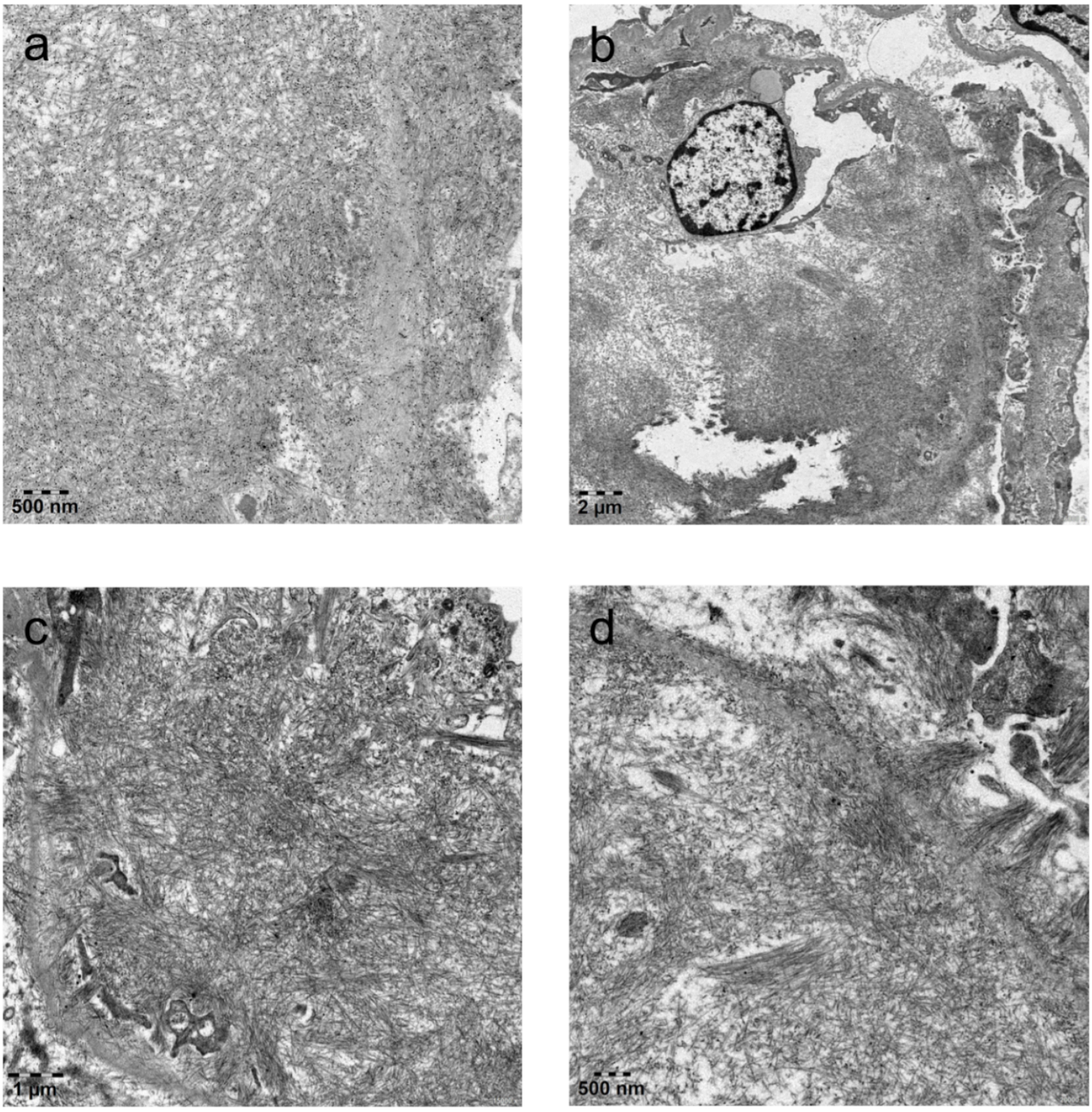


Figure 2

Electron microscopy of the renal biopsy specimen

Immuno-electron microscopy markers: (a)Kappa (-, no colloidal gold particles attached to amyloid fibers), (b) Lambda (-, no colloidal gold particles attached to amyloid fibers), (c) and (d) AA (+, a large amount of colloidal gold particles attached to amyloid fibers)

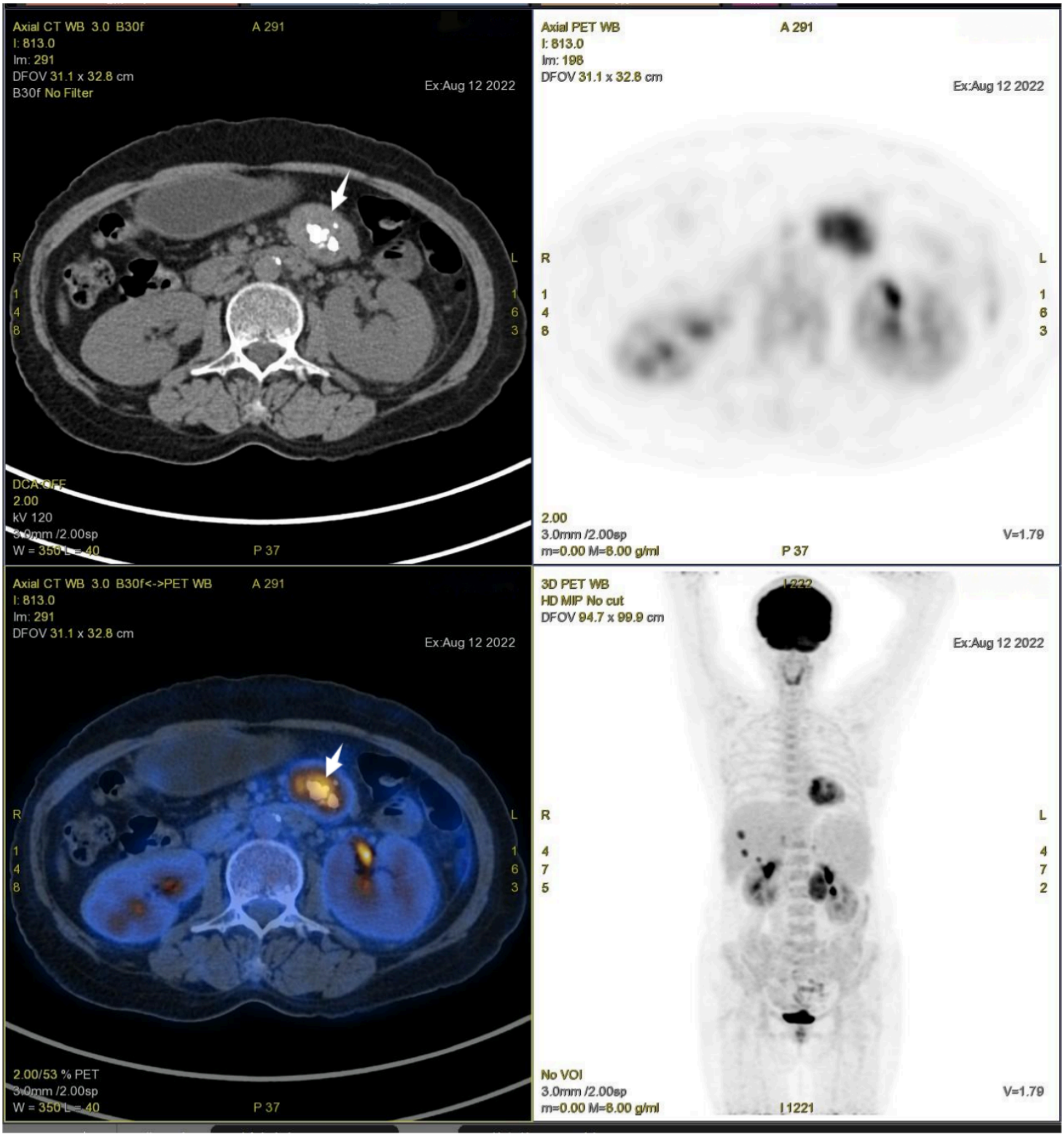


Figure 3

PET-CT scan result

High 18F FDG uptake in the arrowed area, size is approximately 3.1×4.4cm, and the enhanced scan shows uniform enhancement. Multiple punctate/sheet-like calcifications are seen inside, with clear boundaries and smooth edges, and no clear correlation with surrounding organs.

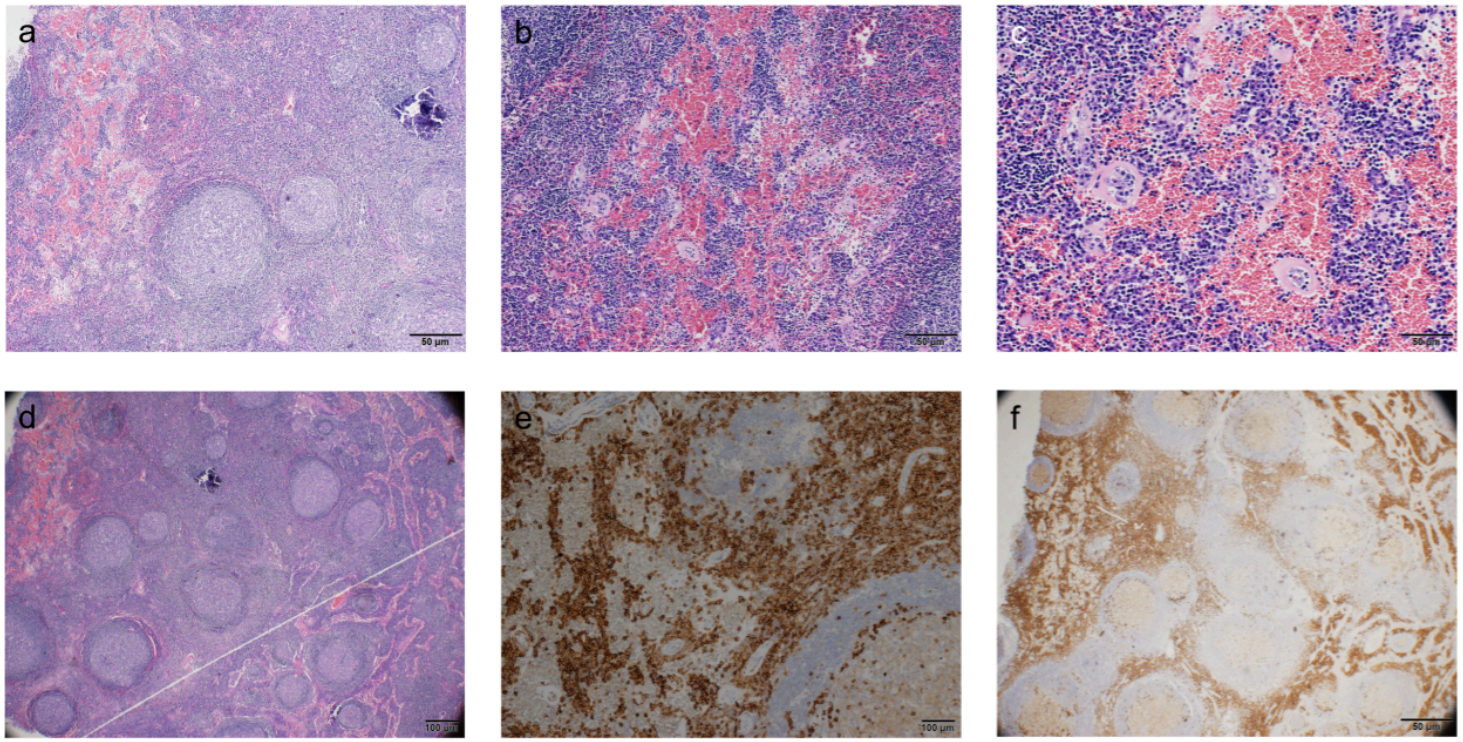


Figure 4

Immunohistochemical staining of the excised lymph node

Panels (a)–(d) show sections stained with hematoxylin and eosin (HE), while panels (e) and (f) show immunohistochemical staining for CD38.

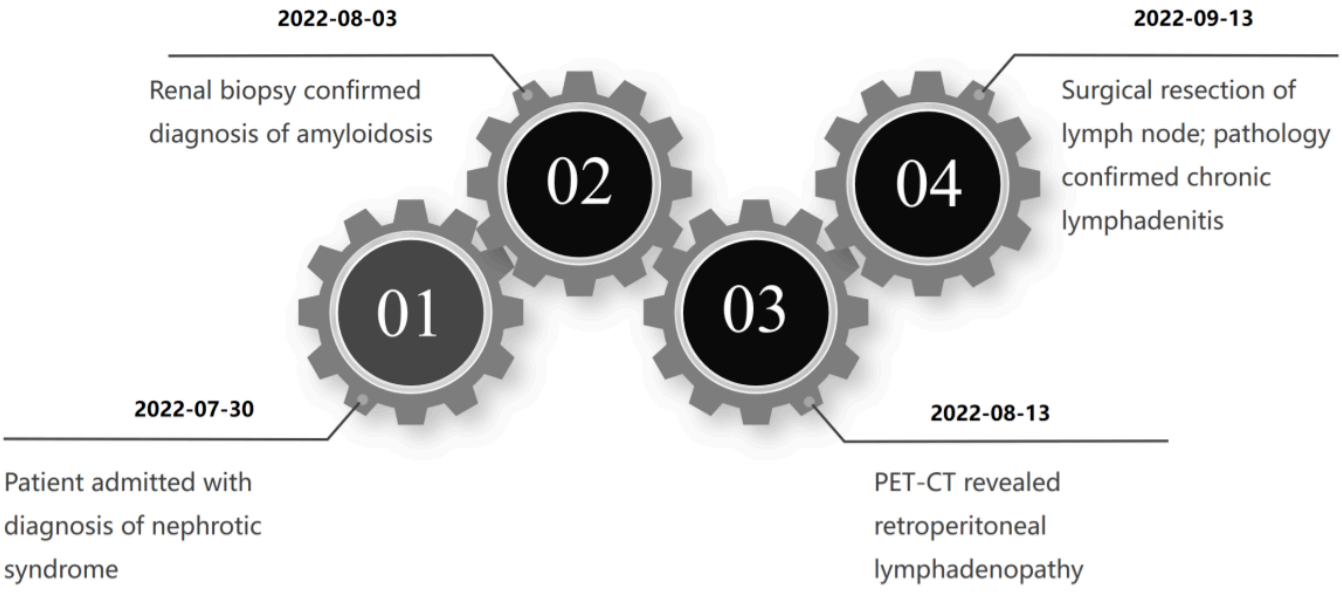


Figure 5

Unnumbered image in the Case presentation section.